NACA

RESEARCH MEMORANDUM

INVESTIGATION AT TRANSONIC SPEEDS OF THE EFFECTS OF INLET LIP STAGGER ON THE INTERNAL-FLOW CHARACTERISTICS

OF AN UNSWEPT SEMIELLIPTICAL AIR INLET

By Gene J. Bingham and Charles D. Trescot, Jr.

Langley Aeronautical Laboratory
Langley Field, Va.

NATIONAL ADVISORY COMMITTEE FOR AERONAUTICS

WASHINGTON

May 1, 1956
Declassified May 2, 1958

NATIONAL ADVISORY COMMITTEE FOR AERONAUTICS

RESEARCH MEMORANDUM

INVESTIGATION AT TRANSONIC SPEEDS OF THE EFFECTS OF INLET

LIP STAGGER ON THE INTERNAL-FLOW CHARACTERISTICS

OF AN UNSWEPT SEMIELLIPTICAL AIR INLET

By Gene J. Bingham and Charles D. Trescot, Jr.

SUMMARY

An investigation has been made in the Langley transonic blowdown tunnel to study the effects of variations in inlet lip stagger from 0° to 60° on the internal-flow characteristics of an unswept semielliptical scoop-type air-inlet model without boundary-layer control. Tests were made at Mach numbers of 1.0, 1.2, and 1.4 through a mass-flow-ratio range from about 0.3 to 0.9 at an angle of attack of 0°.

The test results indicate that, for all angles of inlet lip stagger, part of the boundary layer was bypassed around the inlet lips. As the lip stagger was increased, the boundary layer was more completely bypassed from the region of the rearward lip than from the forward lip. This bypassing was most complete for the 30° stagger inlet and, therefore, the maximum recovery (average total-pressure recovery of 0.95 at a mass-flow ratio of approximately 0.6) was obtained with this configuration. For the 30° stagger inlet, the bypassing effected increases in pressure recovery with decreases in inlet flow rate at Mach numbers of 1.2 and 1.4. When the lip stagger was increased to 45° and then to 60°, the total pressure losses in the region of the forward lip were progressively increased.

At the Mach number where lip stagger had the largest effect on total-pressure recovery, increases in lip stagger from 0° to 30° either had a slight favorable effect (at Mach number of 1.2) or had no effect (at Mach number of 1.4) on the flow distortions at the inlet measuring station. When the lip stagger was increased from 30° to 45° and then to 60°, however, adverse effects of stagger were indicated at all test conditions.

TNTRODUCTION

The results of many investigations of scoop-type air intakes without boundary-layer control devices have indicated that in general the inlet total-pressure recovery tends to decrease as the inlet mass-flow ratio is reduced. (For example, see refs. 1 and 2.) This trend is attributed to the effect of the adverse pressure rise on the growth or separation of the boundary layer ahead of the inlet which becomes more severe as the inlet flow rate is reduced. At supersonic speeds, additional boundary-layer losses are effected by the interaction of the inlet shock with the boundary layer.

The results of a more recent investigation (ref. 3) of the internal-flow characteristics of an unswept scoop inlet which had a lip stagger of 30° have indicated an unusual trend of increasing total-pressure recovery with decreasing inlet mass-flow ratio. Inasmuch as the configuration did not have a fixed boundary-layer control device, this trend was attributed to a "natural" bypassing of some of the fuselage-boundary-layer air around and outside of the downstream lip as a result of the superstream static pressure field immediately ahead of the inlet. The static pressure near the inlet would increase with a decrease in mass-flow ratio for any inlet configuration, but in this case the lip stagger apparently permitted the thickened or separated boundary layer to be diverted around the inlet to the lower pressure field of the fuselage.

A survey of existing data on scoop-type inlets without boundary-layer control devices indicates that these inlets either have little or no lip stagger. (For example, see ref. 1.) For the cases where lip stagger was employed, the inlets were swept. (For example, see ref. 2.) None of these configurations without boundary-layer control had the unusual trend of increasing pressure recovery with decreasing mass-flow ratio obtained in reference 3. Upon consideration of these results along with those of reference 3, it seemed apparent that inlet lip stagger and sweep were important factors affecting the internal-flow characteristics of a scoop-type inlet.

The present investigation was undertaken in the Langley transonic blowdown tunnel to study some of the effects of stagger and sweep on the internal-flow characteristics of a scoop-type inlet. The results of the lip-stagger portion of the investigation are reported in this paper.

For the present tests, the inlet lip stagger was varied from 0° to 60° in increments of 15° . These tests were conducted at Mach numbers of 1.0, 1.2, and 1.4 through a range of mass-flow ratio from about 0.3 to 0.9 at an angle of attack of 0° .

SYMBOLS

H total pressure

p static pressure

 $\frac{H - p_0}{H_0 - p_0}$ impact-pressure ratio

 $\frac{p - p_0}{H_0 - p_0}$ static-pressure ratio

H/Ho integrated inlet total-pressure recovery weighted with

respect to mass flow, $\frac{\int_{A} \frac{\rho V}{\rho_{o} V_{o}} \frac{H}{H_{o}} dA}{\int_{A} \frac{\rho V}{\rho_{o} V_{o}} dA}$

H_{i,max} H_{i,min}

H_o H_o

ratio of maximum inlet total-pressure difference to integrated inlet total-pressure recovery

m_i/m_o mass-flow ratio, defined as ratio of total inlet mass flow to mass flow through free-stream tube with area equal to that of minimum projected frontal area of inlet (0.556 sq in.)

m mass rate of internal flow

M Mach number

V velocity

D diameter, in.

A duct area

ρ mass density, slugs/cu ft

Subscripts:

i inlet

o free stream

max maximum

min minimum

MODEL

A photograph of the model is presented in figure 1 and a side-view drawing of the model is shown in figure 2. The configuration, which was constructed of plastic, consisted of an unswept semielliptical scooptype inlet (table I) mounted on a body of revolution. The forward part of the body was 4.67 inches long with a 1-inch radius at the maximum diameter and was generated by rotating NACA 1-series nose-inlet coordinates about the center line. Downstream of station 4.67 the body was cylindrical (fig. 2). The inlet was symmetrical about the center line (table I) and the ratio of the maximum height to maximum width was 1.5. The inlet lips were approximately semielliptical in shape with a length-thickness ratio of 2.0. The ratio of the minimum inlet area projected on a plane perpendicular to the body axis (0.556 sq in.) to the maximum frontal area of the forebody was 0.177.

During the course of the investigation, the lip stagger was varied from 0° to 60° in increments of 15° with 0° of sweep. The lips were staggered by removing a portion of the rearward lip, but the center line of the plane of the inlet lips was maintained within the limits indicated in figure 3. It was assumed that this small variation in inlet-lip location would have no effect on the inlet-flow characteristics.

The internal-duct-area distribution (exclusive of instrumentation) is shown in figure 4. The duct area was held constant from the inlet to the inlet measuring station behind which the walls diverged at a rate equivalent to that of a 6° conical diffuser and faired into a rectangular duct at station 13.25. Behind this station was located a rectangular-shaped venturi at which the inlet mass-flow ratio was measured. The mass-flow ratio was controlled by varying the area at the exit of the duct.

APPARATUS AND METHODS

Pressure Measurements

The pressure instrumentation at the inlet and venturi measuring stations is shown in figure 2. Twenty total-pressure tubes were located at the inlet along with one static-pressure tube and one orifice located at the fuselage surface (station 7.80). Twenty-five total-pressure tubes were located at the venturi station with two static-pressure tubes and one wall orifice. Static-pressure orifices were distributed along the fuselage vertical center line from station 1.00 on the nose to the inlet measuring station.

Flow Study

Schlieren photographs and an oil-flow technique were used to aid in the study of the nature of the flow ahead of the inlet measuring station. The oil-flow study consisted of placing oil droplets at various points on the surface of the model in and around the inlet and then photographing the paths of the droplets after each run. The pattern made by the oil droplets indicated the flow direction within the boundary layer.

Tests

The tests were conducted in the Langley transonic blowdown tunnel through a mass-flow-ratio range from 0.3 to 0.9 at Mach numbers of about 1.0, 1.2, and 1.4 for an angle of attack of 0°. The maximum mass-flow ratio was limited to 0.91 due to internal blockage. In order to assure that the boundary layer ahead of the inlet was turbulent, an encircling roughness band extending from fuselage station 0.50 inch to 0.75 inch was added to the model nose. This transition strip was made up of 0.003- to 0.005-inch-diameter carborundum grains blown on a thin layer of wet shellac. The tunnel stagnation pressure was held constant at either 50 or 60 pounds per square inch absolute with a resulting Reynolds number varying from about 2.8 x 10⁶ to 3.3 x 10⁶ based on the body diameter of 2 inches. The estimated test accuracy is as follows:

$\frac{H - p_0}{H_0 - p_0} \cdot \cdot \cdot$	 	±0.005
Ħ/H _o		
$\frac{m_{\underline{1}}}{m_{O}}$	 	

RESULTS AND DISCUSSION

Flow Over Fuselage Nose

The static-pressure distributions indicate that for all test conditions local Mach numbers greater than free-stream values existed over the fuselage nose (fig. 5). In fact, at a free-stream Mach number of 1.4, local Mach numbers of 1.48 are indicated. The supersonic velocities ahead of the inlet terminate with a shock wave. For free-stream Mach numbers of about 1.18 and above, schlieren photographs show that this shock was a lambda-type wave for all test configurations. (For example, see fig. 6.) Inasmuch as the transition strip located well forward of the inlet assured that the fuselage boundary layer was turbulent, the lambda-type shock must be associated with turbulent separation. (See ref. 4.) The initial pressure rise ahead of the inlet, therefore, corresponds to the front leg of the lambda. As the lip stagger angle was increased, the distance between the front leg of the lambda (point of separation) and the forward inlet lip tends to decrease whereas the distance to the rear inlet lip generally increases.

Total-Pressure Recovery at Inlet

The average total-pressure recovery at the inlet measuring station is presented in figure 7 for the range of test variables. At a Mach number of 1.0, total-pressure recoveries equal to or greater than 0.97Ho were measured through the range of test mass-flow ratios for all configurations and the variations in pressure recovery with flow rate were small. When the Mach number was increased to 1.2, reductions in pressure recovery were effected in most instances because of interaction of the shock wave located ahead of the inlet and the boundary layer. Variations in pressure recovery with mass-flow ratio were also effected; for the 60° configuration there was a decrease in pressure recovery with decreases in mass-flow ratio while for the 15° and 30° stagger inlets a reverse trend was measured. The maximum variation for these configurations, however, was about 0.02Ho for the range of test mass-flow ratio. At a Mach number of 1.4, the maximum of the tests, the average total-pressure

NACA RM L56C22 7

recovery decreased as the mass flow was reduced for all configurations except for the 30° stagger inlet; for the 30° configuration, however, the reverse trend was again effected. The trend of decreasing recovery with a decrease in mass-flow ratio agrees with that usually obtained with scoop-type inlets without boundary-layer control devices. (For example, see refs. 1 and 2.) This decrease in recovery is associated with increases in boundary-layer losses resulting from a more severe adverse pressure gradient ahead of the inlet as the mass flow is reduced. It was indicated in reference 3 that the unusual trend of increasing recovery with decreasing mass-flow ratio, and indicated herein for the 15° and 30° configurations at $M_0 = 1.2$ and for the 30° configuration at Mo = 1.4, may be attributed to a "natural" bypassing of a large part of the boundary-layer air around the rearward inlet lip. It was concluded in this reference that the amount of boundary-layer air bypassed probably increased with reductions in mass-flow ratio as a result of the increase in inlet static pressure with reductions in flow rate. This increase in inlet static pressure would result in a greater pressure differential between the inlet flow and external flow and would permit a greater amount of separated boundary layer to flow to the lower pressure field on the fuselage.

In order to show more clearly the flow phenomenon involved for the various inlet configurations of the present tests, contours of constant impact-pressure ratio at the inlet measuring station are presented in figure 8 for the test range, and photographs of the oil flow patterns are shown in figure 9 for a Mach number of 1.4. These flow patterns are typical of those obtained at all test Mach numbers.

With the 00 stagger configuration installed, it is indicated (fig. 8(a)) that, in general, the maximum values of impact-pressure ratio and the areas of high recovery decrease as the mass-flow rate is reduced from the highest to the lowest value for all Mach numbers. This decrease might have been expected since, as previously pointed out, the pressure gradient ahead of the inlet becomes more severe at the low mass-flow ratios and effects increases in boundary-layer thickness. There is a tendency, however, for the pressure losses in the regions adjacent to the body surface to decrease as the mass-flow ratio is reduced. The oil flow patterns for the 0° stagger inlet (for example, see fig. 9(a)) indicated that, for all test conditions, the boundary-layer air separates ahead of the inlet and is diverted, to some extent, around both inlet lips. Although not shown in the photograph, the point of reattachment was slightly inside the inlet plane. It seems apparent, then, that part of the boundary layer is being bypassed in a manner similar to that previously mentioned for the 30° staggered inlet of reference 3 for which bypassing of the boundary layer was most complete at the low mass-flow ratios. In the

present case of 0° stagger, however, the amount of boundary layer bypassed was not great enough to effect increases in average total-pressure recovery with decreases in mass-flow ratio.

It will be noted that both the impact-pressure contours and the oil patterns show that the flow was approximately symmetrical about the inlet center line.

When the lip stagger was increased to 15°, the impact-pressure distributions (fig. 8(b)) indicate that more of the boundary-layer air ahead of the inlet measuring station was bypassed than for the 0° stagger configuration and that increases in average total-pressure recovery (fig. 7) were effected at the various test conditions. The improvement was sufficient to result in a small increase in average total-pressure recovery with a decrease in mass-flow ratio at Mach numbers of 1.0 and 1.2.

When the inlet lip stagger was again increased, this time from 15° to 30°, further reductions in boundary-layer thickness at the inlet measuring station were indicated by the impact-pressure-ratio contours (fig. 8(c)) along with a corresponding increase in average total-pressure recovery (fig. 7). The boundary layer, therefore, must be more completely bypassed than it was for either the 0° or 15° stagger case. As was previously mentioned, the axial static-pressure distributions ahead of the inlet measuring station (fig. 5) indicate that the distance between the inlet shock and the rearward inlet lip increases as the lip is staggered from 0° to 30°; the boundary layer, therefore, has more space in which to be bypassed. It would seem, therefore, that because of this increase in distance, the boundary layer is more easily bypassed around the rearward inlet lip.

As continuity requires, increases in inlet total-pressure recovery effected by staggering the inlet lips from 0° to 30° are accompanied by increases in inlet static-pressure ratio (for constant mass-flow ratio) (fig. 5). These increases in inlet static pressure, of course, influence the bypassing of the boundary layer.

As previously pointed out, increases in average pressure recovery with decreases in mass-flow ratio were effected for the 30° staggered inlet at a Mach number of 1.4 at mass-flow ratios greater than 0.63. When the mass-flow ratio was reduced below this value, however, there was a reduction in pressure recovery. For these lowest mass-flow conditions, the boundary-layer losses become so great that the inlet cannot bypass enough of the low-energy air to maintain the trend measured at slightly higher mass-flow ratios.

J

It is indicated in figure 8(c) that there is, in general, a tendency for the impact-pressure ratios to be somewhat higher adjacent to the rearward lip than they are in the regions of the forward lip. This tendency is attributed to the fact that a greater part of the boundarylayer air is bypassed from the region of the rearward lip; the boundarylayer losses, therefore, are greatest next to the forward lip, especially at a Mach number of 1.4. The closeup photographs of the oil flow patterns (for example, see fig. 9(b)) show that these losses can be attributed to a rapid growth of the separated boundary layer along the inner surface of the forward lip. In fact, the oil patterns indicate that the separated region at the inner surface exceeds one-half of the inlet height. This boundary-layer growth must be associated with the continuation of the longitudinal adverse pressure gradient back to the position of the rearward lip. (See fig. 5.) Observation of figure 8(b) indicates that in some instances differences similar to those just discussed were effected for the 150 stagger inlet. These differences, however, were small.

When the lip stagger was increased from 30° to 45° and then to 60°, these total-pressure losses in the region of the forward lip were progressively increased. For these higher stagger angles, the growth of the separated boundary layer with decreasing mass-flow ratio eliminated the trend of increasing recovery with decreasing mass-flow ratio, even though the oil flow patterns (fig. 9) indicate that a large part of the fuselage boundary layer was being bypassed around the rearward lip. It can be seen in figure 7 that the average total-pressure recovery of the 60° stagger inlet was less than that of any other configuration at supersonic speeds.

The effects of lip stagger on the average total-pressure recovery are summarized in figure 10 where pressure recovery is plotted as a function of the lip stagger for several mass-flow ratios at Mach numbers of 1.0, 1.2, and 1.4. Here it is again seen that, at a Mach number of 1.0. total-pressure recoveries equal to or greater than 0.97Ho were measured through the range of mass-flow ratio for all configurations, and the variations in pressure recovery with flow rate were small. At Mach numbers of 1.2 and 1.4, the effects of lip stagger are more important. For example, increasing the lip stagger from 0° to 30° at a Mach number of 1.2 caused an increase in pressure recovery from about 0.96Ho to 0.99Ho at a mass-flow ratio of 0.5. The recovery is reduced to about 0.91Ho, however, when the stagger is increased from 300 to 600 at these same operating conditions. Variations in lip stagger were less influential at a mass-flow ratio of 0.8. When the test Mach number was increased to 1.4, stagger became slightly more influential at the low flow rates. For this case, increasing lip stagger from 0° to 30° corresponds to an increase in recovery from about 0.89Ho to 0.95Ho at a mass-flow ratio of 0.6, while for 600 the recovery was reduced to

NACA RM L56C22

about 0.82H $_{0}$. In view of the fact that the inlets did not have a boundary-layer control device, it is of particular interest to note that the 30 $^{\circ}$ stagger configuration produced near-normal shock recovery (0.958H $_{0}$ at M $_{0}$ = 1.4) at a mass-flow ratio of 0.6. This result is of special interest since, as previously pointed out, local Mach numbers greater than stream values were indicated ahead of the inlet shock wave for all test conditions.

Flow Distortions at Inlet

The impact-pressure distributions (fig. 8) indicate that in some instances a large variation in total-pressure existed over the inlet measuring station. In order to show the effects of lip stagger and mass-flow ratio on the variation of inlet total-pressure across the inlet, the ratio of the maximum local total-pressure difference to the average total-pressure recovery is presented in figure 11 as a function of mass-flow ratio for the various test configurations at Mach numbers of 1.0, 1.2, and 1.4.

At the Mach numbers where lip stagger had the largest effect on total-pressure recovery, increases in lip stagger from 0° to 30° either had a slight favorable effect ($M_0 = 1.2$) or had no effect ($M_0 = 1.4$) on the flow distortions at the inlet measuring station. When the lip stagger was increased from 30° to 45° and then to 60°, however, adverse effects of stagger were indicated at all test conditions. It can be seen in figure 11 that the minimum distortion was usually effected at the low mass-flow ratios which, in the case of the 30° stagger inlet, is in the range of maximum recovery. The reasons for this trend are shown in figure 8. Here it is seen that there is generally a simultaneous decrease in the maximum local recovery and an increase in minimum local recovery with decreases in mass-flow ratio.

A secondary flow is indicated by the oil flow patterns (figs. 9(b) and 9(c)) which, as previously pointed out, has adverse effects on the total-pressure recovery at the inlet and also has adverse effects on the inlet flow distortions. It is believed that some type of boundary-layer control, such as a simple slot at the lip-fuselage juncture, could alleviate the secondary flow and thus improve the inlet flow distortions.

Inlet-Design Considerations

The results of this study indicate that, from the standpoint of both pressure recovery and inlet flow distortions, a scoop-type inlet similar to that investigated should incorporate approximately 30° of lip stagger and should be designed for operation near a mass-flow ratio of 0.63 at $M_{\circ} = 1.4$. When it is realized, however, that the overall inlet

performance depends upon the external drag as well as the pressure recovery and flow distortions, the optimum design mass-flow ratio is not so obvious. Inasmuch as the maximum total-pressure recovery for the 30° stagger inlet was measured at $\rm m_1/m_0\approx 0.63~(M_0=1.4)$ and inasmuch as the minimum drag would be obtained at a mass-flow ratio nearer unity, the maximum thrust minus drag would probably occur at some intermediate inlet flow rate. The optimum design point, therefore, would naturally depend upon the spillage drag characteristics of the particular installation, that is, the slope of the drag curve with respect to mass-flow ratio. In order to realize the maximum possible advantage of the increase in inlet total-pressure recovery with decreasing mass flow exhibited by the 30° stagger inlet, the configuration must be designed so that the increase of drag with a decrease in mass-flow ratio is relatively low.

CONCLUSIONS

An investigation has been made in the Langley transonic blowdown tunnel to study the effects of variations in inlet lip stagger from 0° to 60° on the internal-flow characteristics of an unswept semielliptical scoop-type inlet model. Tests were made at Mach numbers of 1.0, 1.2, and 1.4 through a mass-flow ratio range from about 0.3 to 0.9 at an angle of attack of 0°. The more important results are summarized as follows:

- l. For all angles of inlet lip stagger, part of the boundary layer was bypassed around the inlet lips. As the inlet lip stagger was increased, the boundary layer was more completely bypassed from the regions of the rearward lip than from the forward lip.
- 2. The maximum recovery was obtained with the 30° stagger inlet (average total-pressure recovery of 0.95 at a mass-flow ratio of approximately 0.6). For this configuration, the bypassing effected increases in pressure recovery with decreases in inlet flow rate at Mach numbers of 1.2 and 1.4.
- 3. When the lip stagger was increased to 45° and then to 60°, the total-pressure losses in the region of the forward lip were progressively increased. The average total-pressure recovery of these two configurations was less than that of the 30° stagger inlet because of the entrance of the boundary layer.
- 4. At the Mach numbers where lip stagger had the largest effect on total-pressure recovery, increases in lip stagger from 0° to 30° either had a slight favorable effect (at Mach number of 1.2) or had no effect (at Mach number of 1.4) on the flow distortions at the inlet

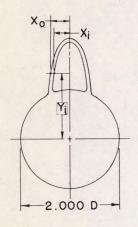
measuring station. When the lip stagger was increased from 30° to 45° and then to 60°, however, adverse effects of stagger were indicated at all test conditions.

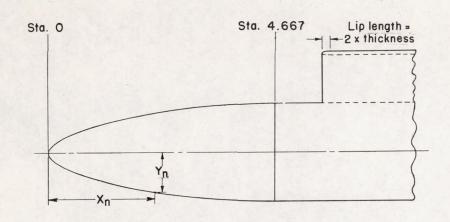
Langley Aeronautical Laboratory,
National Advisory Committee for Aeronautics,
Langley Field, Va., March 5, 1956.

REFERENCES

- 1. Frazer, Alson C., and Anderson, Warren E.: Performance of a Normal-Shock Scoop Inlet with Boundary-Layer Control. NACA RM A53D29, 1953.
- 2. Howell, Robert R., and Trescot, Charles D., Jr.: Investigation at Transonic Speeds of Aerodynamic Characteristics of a Semielliptical Air Inlet in the Root of a 45° Sweptback Wing. NACA RM L53J22a, 1953.
- 3. Bingham, Gene J.: Investigation at Transonic Speeds of the Aerodynamic Characteristics of an Unswept Semielliptical Air Inlet in the Root of a 45° Sweptback Wing. NACA RM L55F22a, 1955.
- 4. Nussdorfer, T. J.: Some Observations of Shock-Induced Turbulent Separation on Supersonic Diffusers. NACA RM E51126, 1954.

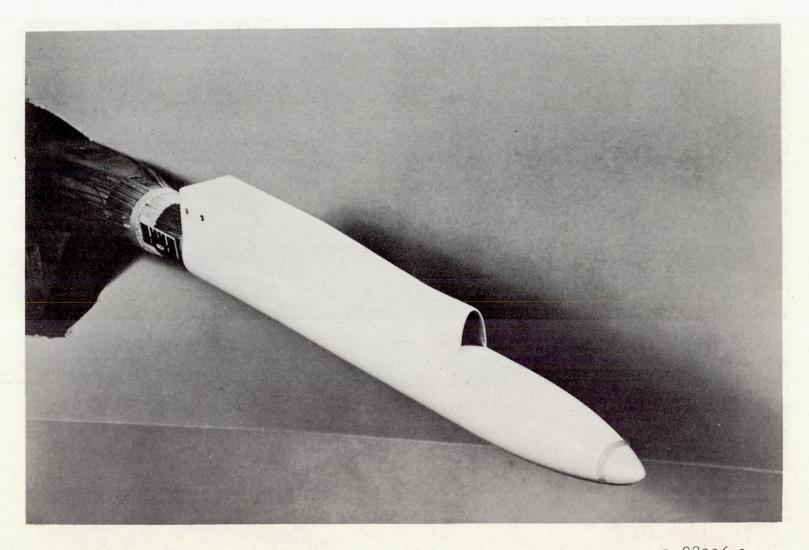
TABLE I. - DESIGN COORDINATES FOR NOSE AND INLET SECTIONS



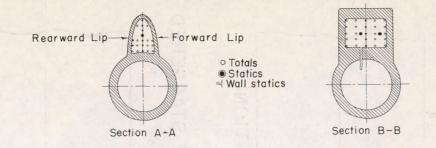


	Coordinates for						
	inlet section						
Y	Yi		Xi		0		
0.9				0.4			
.9	60	0.3	15	. 4	29		
.9	80	. 3	43 54 52 50 44 32 18 01 77 46 05 80 42 29 05	. 4	29		
1.0	00	.3	54	. 4	29		
1.0	50	. 3	52	.4	29		
1.1	00	. 3	50	.4	25		
1.2	00	.3	44	.4	19		
1.3	00	. 3	32	.4	07 93 76 52 25 85 67		
1.4	00	.3	18	. 3	93		
1.5	00	. 3	01	. 3	76		
1.6	00	.2	77	. 3	52		
1.7	00	.2	46	. 3	25		
1.8	00	.2	05	.2	85		
1.8	50	.1	80	.2	67		
1.9	00	. 1	42	.2	40		
1.9	25		29	. 2	23 05		
1.9	50	. 1	05	.2	Q5		
1.9 1.9 1.9 1.9	60	.0	90 72				
1.9	70	.0	72				
1.9	80	.0	65 42				
1.9	90	.0	42				
2.0	00.	.0	00		55		
2.0	25		-	. 1	30		
2.0	50			.0	80		
2.0	15			. 0	00		

Coordinates for					
nose contour					
Xn	Yn				
0 000	0.000				
019	.066				
.037	.093				
.047	.104				
.070	.127				
.093	.147				
.093	.066 .093 .104 .127 .147 .183 .215 .244 .295 .340				
.187	.215				
.233	.244				
.327	.295				
.420	.340				
.560	.401				
.700	.453 .527 .592				
.933	.527				
.327 .420 .560 .700 .933 I.167 I.400 I.866 2.333	.592 .649 .748 .827				
1.400	.649				
1.866	.748				
2.333	.827				
2.706	.880				
2.986	.912				
3.173	.931				
2.706 2.986 3.173 3.546 3.919	.880 .912 .931 .962 .983				
3.919	.983				
4.293	.997				
4.667	1.000				



L-88096.1 Figure 1.- Three-quarter front view of 0° stagger inlet model.



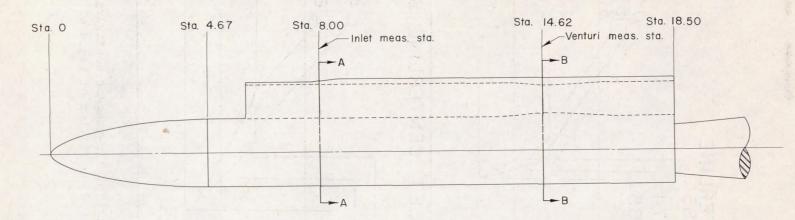


Figure 2.- View of model showing internal ducting and total-pressure measuring stations. (All dimensions are in inches.)

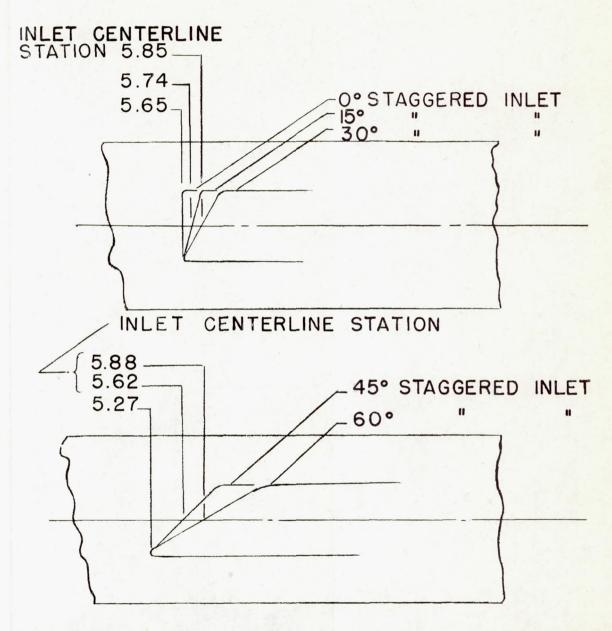


Figure 3.- Sketch of lip-stagger configurations showing fuselage-centerline station of plane of inlet lips.

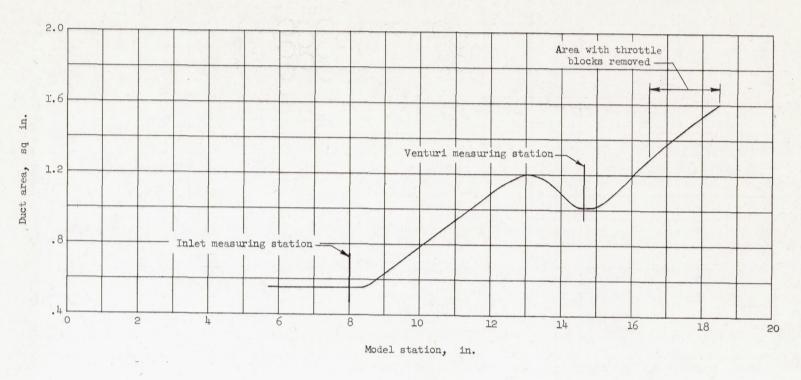


Figure 4.- Internal-duct-area distribution.

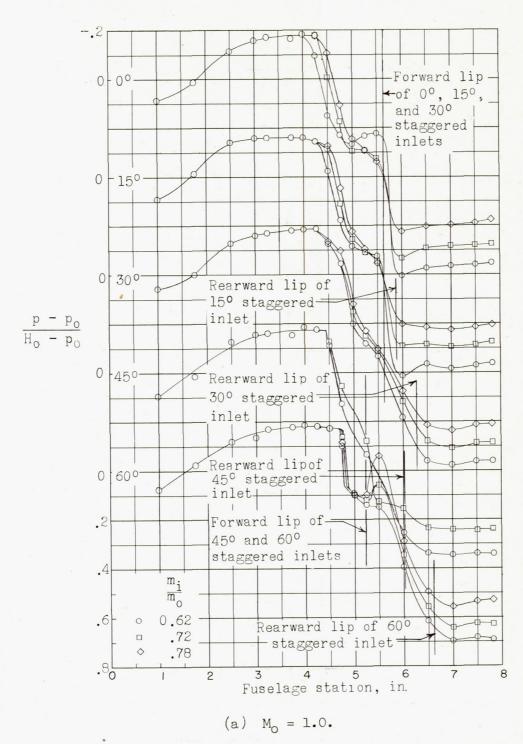


Figure 5.- Surface static-pressure distributions along nose and extending from the inlet plane to the inlet measuring station.

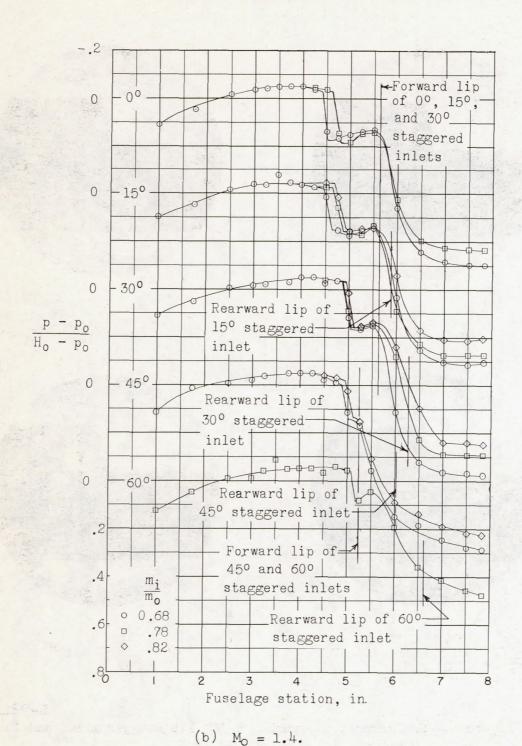


Figure 5. - Concluded.

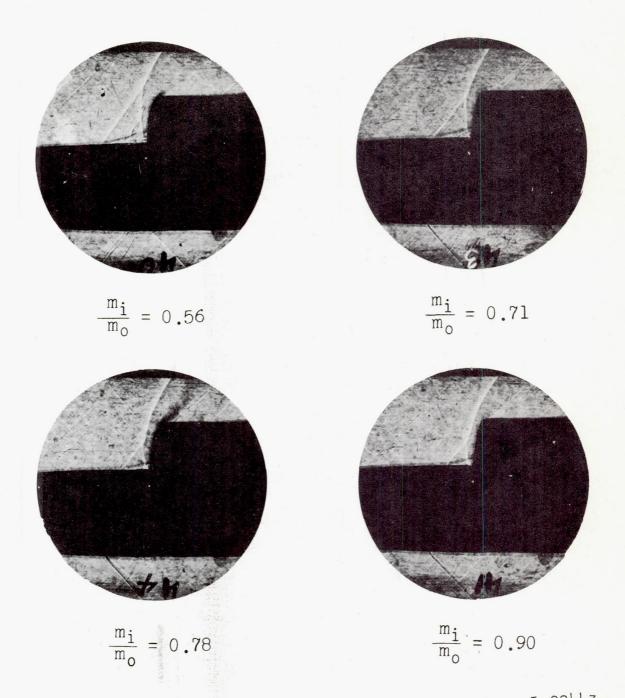


Figure 6.- Schlieren photographs of 30° lip stagger inlet model. $M_{\circ} = 1.4$.

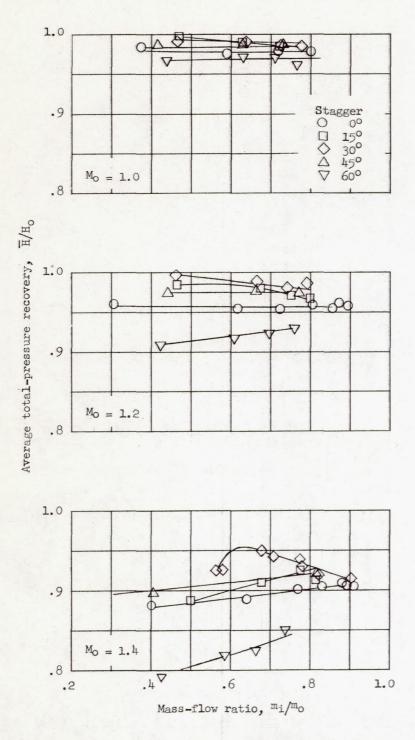
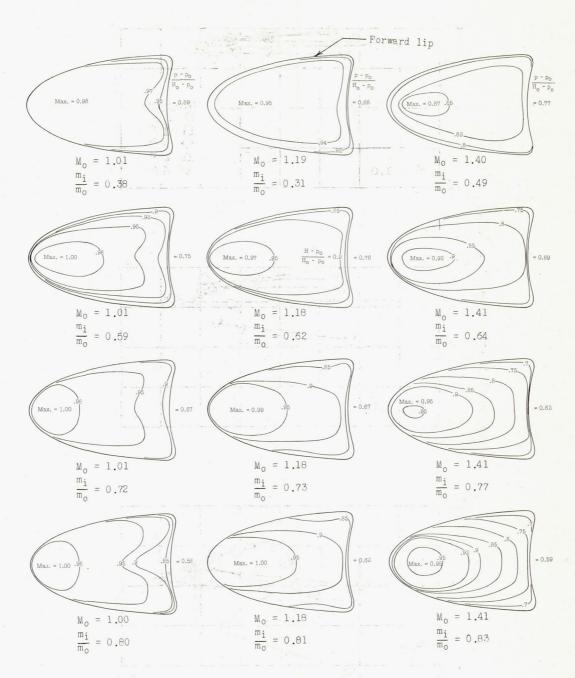


Figure 7.- Effect of variations in mass-flow ratio, Mach number, and lip stagger on total-pressure recovery at inlet measuring station.

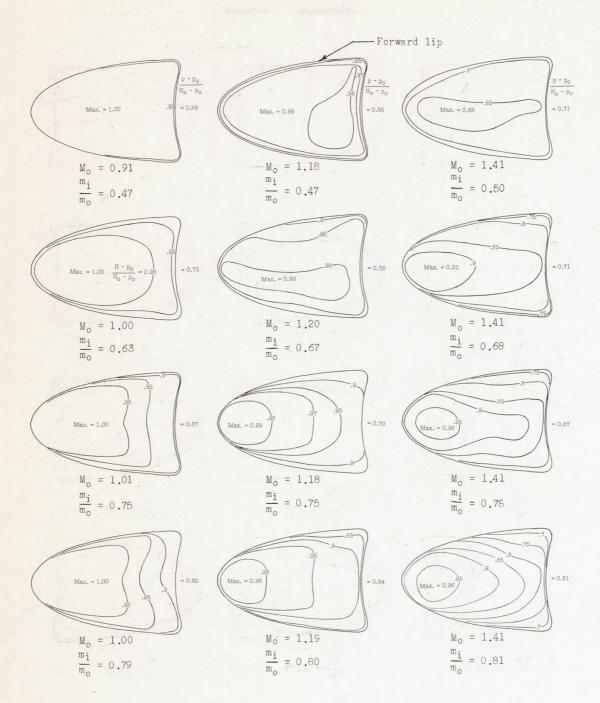


(a) 0° inlet lip stagger.

Figure 8.- Contours on impact-pressure ratio at inlet measuring station at 0° angle of attack.

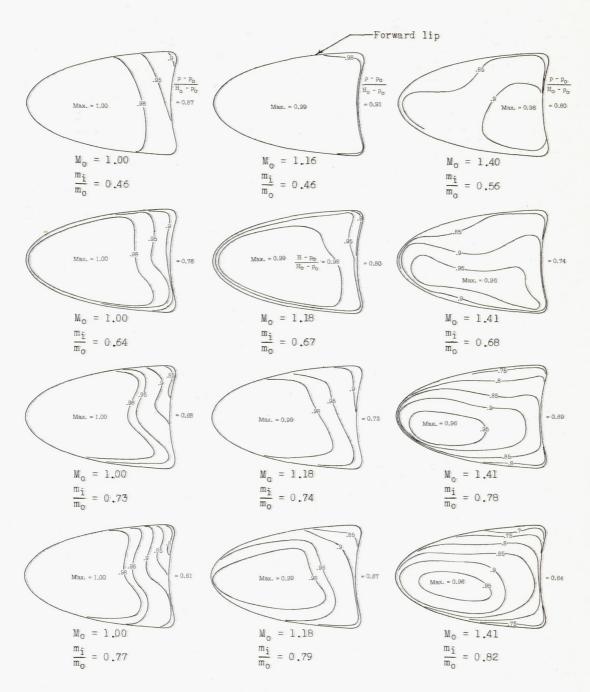
SALALAN ABTRACTOR STATES TO THE

NACA RM L56C22



(b) 15° inlet lip stagger.

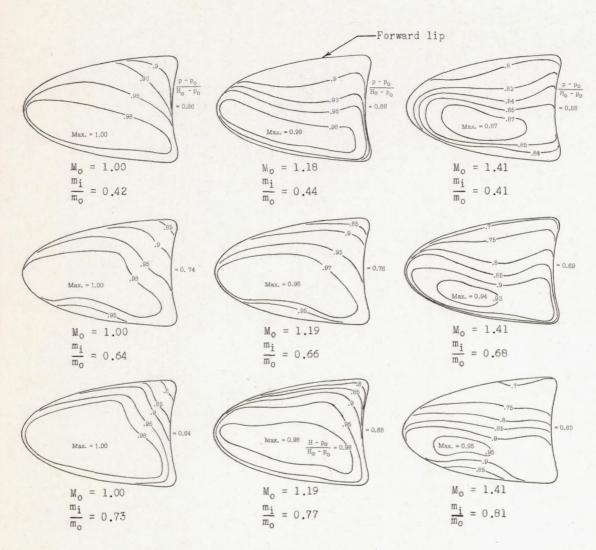
Figure 8. - Continued.



(c) 30° inlet lip stagger.

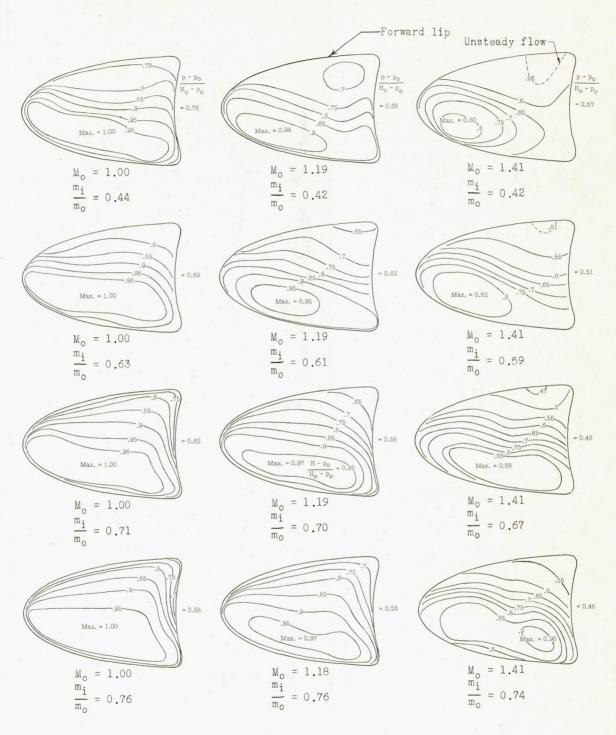
Figure 8. - Continued.

J



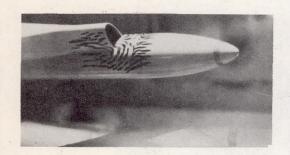
(d) 45° inlet lip stagger.

Figure 8. - Continued.



(e) 60° inlet lip stagger.

Figure 8.- Concluded.



0° stagger



30° stagger



600 stagger



15° stagger

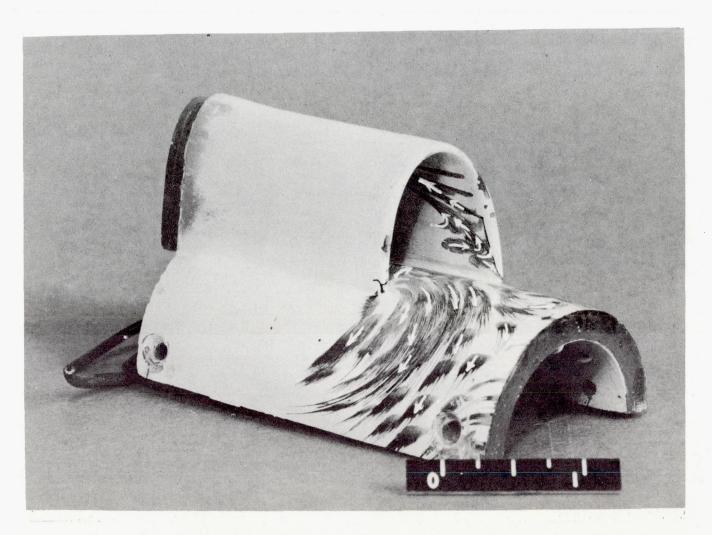


45° stagger

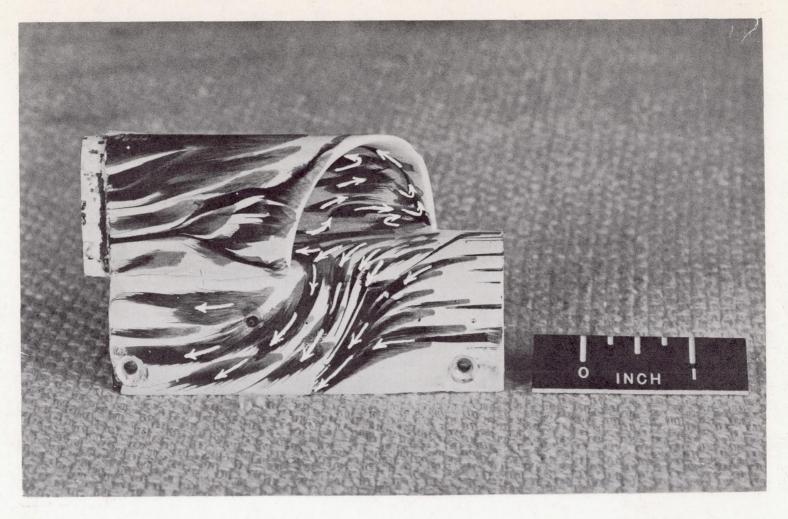
L-92444

(a) Effect of stagger on oil flow patterns.

Figure 9.- Oil-flow-study photographs indicating direction of boundary-layer flow. $M_0 = 1.4$; $m_1/m_0 \approx 0.68$.



(b) Closeup view of 30° stagger inlet. $M_0 = 1.4$; $m_1/m_0 = 0.78$. Figure 9.- Continued.



L-88325.1

(c) Closeup view of 60° stagger inlet. $M_{\odot} = 1.40$; $m_{1}/m_{\odot} = 0.67$.

Figure 9. - Concluded.

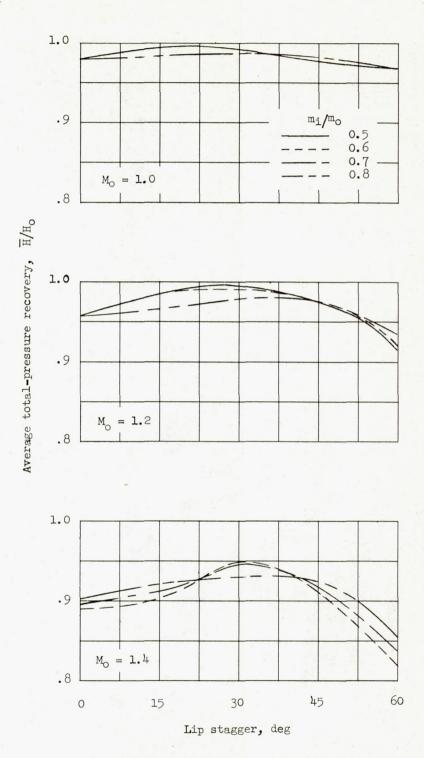


Figure 10. - Comparison of variation of total-pressure recovery with lip stagger for several mass-flow ratios and Mach numbers.

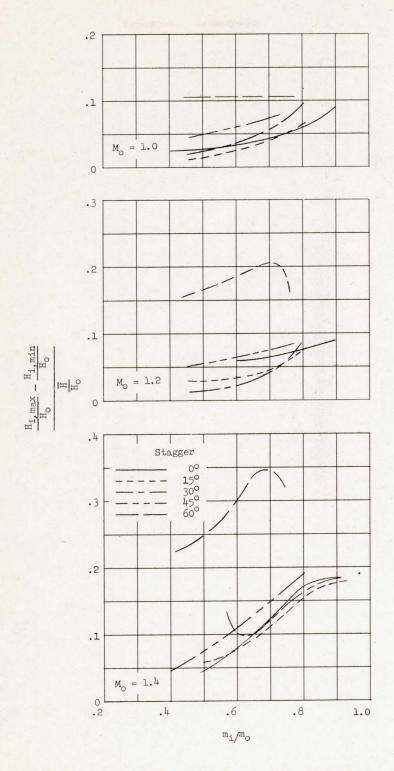


Figure 11. - Effect of variations with mass-flow ratio, Mach number, and lip stagger on the flow distortion at the inlet measuring station.